

## RESULTS OF A RETROSPECTIVE PREDICTION OF PAST STRONG MAINSHOCKS IN THE BROADER AEGEAN AREA BY APPLICATION OF THE ACCELERATING SEISMIC DEFORMATION METHOD

C. B. Papazachos, G. F. Karakaisis and E. M. Scordilis

Department of Geophysics, School of Geology, Aristotle University, Thessaloniki 54124, Greece

Corresponding author: C.B. Papazachos, e-mail: [costas@lemnos.geo.auth.gr](mailto:costas@lemnos.geo.auth.gr)

### ABSTRACT

Accelerated seismic deformation following a time-to-failure power-law is widely believed to culminate with the occurrence of a mainshock, which is typically considered as a critical phenomenon. This critical earthquake concept together with the time-to-failure power-law, expressed through a quantification of the accelerating Benioff strain release, and the recently defined properties of the parameters of this model form the so called "accelerating seismic deformation method" which has been proposed for an intermediate earthquake prediction.

This method is reviewed and applied for a retrospective prediction of eighteen strong mainshocks, which occurred in Greece and the surrounding area in the period 1950-2000. Comparison between observed and predicted parameters indicates that an ensuing mainshock may be predicted by this method with an uncertainty of about 110km for the epicenter,  $\pm 1.5$  years for the origin time and  $\pm 0.4$  for the moment magnitude with high probability (>90% confidence). Some practical problems concerning the real prediction of future earthquakes are discussed.

**Key words:** accelerating seismic deformation, Aegean area

### INTRODUCTION

Accelerating intermediate magnitude seismicity before strong mainshocks has been observed in several regions during the last few decades (Gutenberg and Richter, 1954; Tocher, 1959; Mogi, 1969; Ellsworth et al., 1981; Raleigh et al., 1982; Papadopoulos, 1986; Sykes and Jaume, 1990; Karakaisis et al., 1991; Knopoff et al., 1996; Tzannis et al., 2000). Systematic investigation of this accelerating seismicity has been carried out during the last decade and several physical mechanisms have also been proposed to interpret this phenomenon (Sykes and Jaume, 1990; Bufe and Varnes, 1993; Saleur et al., 1996; Turcotte, 1999; Jaume and Sykes, 1999). The process of generation of moderate magnitude shocks (preshocks) has been recently considered as a critical phenomenon, leading to the generation of large earthquakes (mainshocks), which can be considered as a critical point (Sornette and Sornette, 1990; Sornette and Sammis, 1995; Saleur et al., 1996; Huang et al., 1998). This concept, which is based on principles of statistical physics, interprets fairly well the related seismological observations. One of the most important consequences of this model is that the time variation of measures of preshock – mainshock seismic crustal deformation (seismic energy, seismic moment, Benioff strain) follows a power law. On the basis mainly on this model several attempts have already been made to predict mainshocks (Varnes, 1989; Sykes and Jaume, 1990; Sornette and Sammis, 1995; Bufe et al., 1994).

Bufe and Varnes (1993) proposed the so called time-to-failure power-law method and used as a measure of the preshock seismicity the cumulative Benioff strain,  $S(t)$ , defined as

$$S(t) = \sum_{i=1}^{n(t)} E_i(t)^{1/2} \quad (1)$$

where  $E_i$  is the seismic energy of the  $i$ th preshock and  $n(t)$  is the number of events at time  $t$ . To fit the time variation of the cumulative Benioff strain they proposed a relation of the form:

$$S(t) = A + B(t_c - t)^m \quad (2)$$

where  $t_c$  is the origin time of the mainshock and  $A$ ,  $B$ ,  $m$  are parameters which can be calculated by the available data. The seismic energy,  $E$ , in relation (1) is calculated by appropriate equations which relate this energy with the magnitude of the earthquakes. Bowman and his

colleagues (1998) applied an algorithm to identify circular regions approaching criticality, mainly along the San Andreas fault system since 1950 by minimizing a curvature parameter,  $C$ , which quantifies the degree of acceleration of the Benioff strain. This parameter was defined as the ratio of the root-mean square error of the power-law fit (relation 2) to the corresponding linear fit error. Thus,  $C$  is less than 1 for accelerating or decelerating seismicity and equals to or larger than 1 for a linear variation of seismicity.

During the last three years a systematic work has been carried out on the model expressed by relation (2) by using data for shallow earthquakes in the Aegean area, by imposing additional constraints to the model and by identifying elliptical preshock (critical) regions. This led to an algorithm, which can be used for estimation of the epicenter, magnitude and origin time of ensuing mainshocks (Papazachos and Papazachos, 2000, 2001; Papazachos, 2001). This procedure is called "method of accelerating seismic crustal deformation" because the Benioff strain used in relation (2) is considered as a measure of seismic deformation.

In the present paper an attempt is made to apply this method for retrospective prediction of strong shallow mainshocks (Fig. 1), which occurred in the Aegean area ( $34^{\circ}\text{N} - 42^{\circ}\text{N}$ ,  $19^{\circ}\text{E} - 30^{\circ}\text{E}$ ) between 1950 and 2000. We can then compare the predicted with the observed parameters of these mainshocks in order to have an estimation of the uncertainties in the predicted by this method epicenter coordinates, magnitude and origin time of ensuing mainshocks.

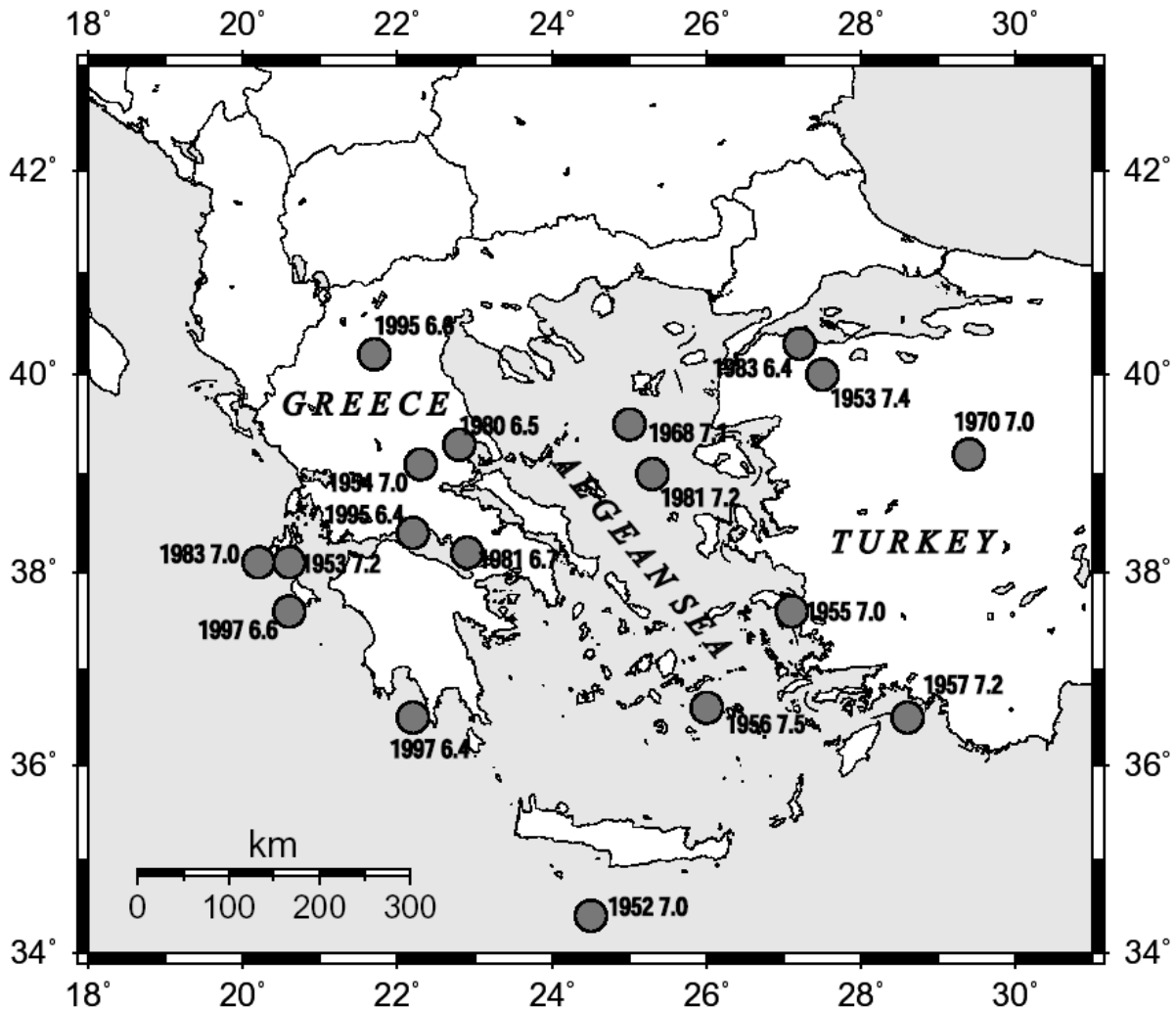


Figure 1. The epicenters of the eighteen strong shallow mainshocks studied in the present work. For each event its year of occurrence and magnitude is given.

### PROPERTIES OF THE ACCELERATING DEFORMATION MODEL

In addition to the basic law expressed by relation (2), the model of preshock seismic deformation has several other properties, which have been recently identified. Thus, Papazachos and Papazachos (2000, 2001) used elliptical instead of circular regions of each considered mainshock and defined several relations, which have been used as additional constraints for the model expressed by relation (2). They derived the following three relations between the magnitude,  $M$ , of the mainshock and the radius,  $R$  (in km), of the circle with area equal to the area of the critical elliptical region, the parameter  $B$  of relation (2) and the average magnitude,  $M_{13}$ , of the three largest preshocks:

$$\log R = 0.41M - 0.64, \quad \sigma = 0.05 \quad (3)$$

$$\log B = 0.64M + 3.27, \quad \sigma = 0.16 \quad (4)$$

$$M = 0.85M_{13} + 1.52, \quad \sigma = 0.21 \quad (5)$$

Similarly, the following two constraints have been defined for the total duration,  $t_p$  (in years), of the preshock sequence:

$$\log t_p = 5.81 - 0.75 \log s_r, \quad \sigma = 0.17 \quad (6)$$

$$A = S_r t_p \quad (7)$$

where  $S_r$  (in Joule<sup>1/2</sup>/yr) is the long-term Benioff strain rate, expressing the average strain energy release in the examined area and  $s_r$  is the same quantity reduced to an area of  $10^4$  km<sup>2</sup>.

The values of the curvature parameter,  $C$ , and of the parameter  $m$  of relation (2) must be quite smaller than 1 in order to have a recognizable accelerating seismicity in the preshock (critical) region. In the previous studies the values of these two parameters have been constrained to be smaller than 0.7 when the center of the elliptical critical region coincides with the mainshock epicenter. Larger values of these parameters indicate that the power-law fit is practically indistinguishable from the linear fit (similar rms errors for both fits or almost linear behavior of the power-law) and consequently the accelerating activity is difficult to be identified (Bowman et al., 1998; Jaume et al., 2000). Therefore any optimization for the determination of the power-law parameters is performed under the following constrains:

$$C \leq 0.7, \quad m \leq 0.7 \quad (8)$$

To quantify the compatibility of the values of the parameters  $R$ ,  $B$ ,  $M$ ,  $t_p$  and  $A$  calculated for a seismic sequence with those determined by relations (3), (4), (5), (6) and (7), a parameter  $P$  was defined (Papazachos and Papazachos, 2001), which is the average value of the probabilities that each of the left-side parameters in these equations attains a value close to its expected one from these relations, assuming that the observed deviations of each parameter follow a Gaussian distribution. Furthermore, the quantity  $q = P/(m \cdot C)$  has been adopted (Papazachos et al., 2002) as a measure of the "quality" of each solution. Using  $P$  and  $q$  as additional criteria for strong earthquakes in the Aegean area and considering as centers of the elliptical critical region not only the mainshock epicenter but also neighboring points resulted in the following cut off values:

$$C \leq 0.60, \quad m \leq 0.35, \quad P \geq 0.45, \quad q \geq 3.0 \quad (9)$$

The accelerating seismic deformation behavior, following relations (2, 3, 4, 5, 6, 7, 8), can not be identified until a time,  $t_i$ , before the occurrence of the mainshock when this behavior is more pronounced, which can be described as the identification time for this phenomenon. Papazachos and his colleagues (2001) showed that the difference,  $t_c - t_i$ , between the identification time and the origin time of the mainshock is of the order of some years ( $3.7 \pm 1.6$  years) and is given by relation:

$$\log(t_c - t_i) = 5.04 - 0.75 \log s_r, \quad \sigma = 0.18 \quad (10)$$

That is, the identification period is larger for low-seismicity areas. From relations (6) and (10) it comes out that:

$$t_c - t_i = (0.17 \pm 0.05)t_p \quad (11)$$

The identification period defined by this relation is almost identical to the results derived independently by Yang and his colleagues (2001), who suggested that when we reach the final 1/6 (~17%) of the total preshock window can the preshock region be identified. Relations (10,

11) can be used to further constrain the origin time of an oncoming mainshock, since  $s_r$  and  $t_p$  can be estimated by the available data at the identification time.

## METHOD AND DATA

To identify a preshock (critical) region shocks (preshocks) with epicenters in an elliptical region centered at a certain geographical point (epicenter of an occurred or oncoming mainshock) are considered and initial values for the parameters (A, B, m) of relation (2), as well as the curvature parameter C are calculated. This is repeated for several values of the azimuth,  $z$ , of the large ellipse axis (e.g. in steps of  $20^\circ$ ), of the length,  $a$ , of this axis (e.g. in steps of 20km), of the ellipticity,  $e$  (e.g. values between 0.6 and 0.95), of the preshock time,  $t_p$  (e.g. in steps of one year), of the mainshock origin time,  $t_c$  (e.g. in steps of one year) and of the mainshock magnitude (e.g. values between  $M_{\min}=5.8$  and the  $M_{\max}$  of the investigated area). These computations are repeated for a grid of points in which the investigated area is separated with the desired density (e.g. with spacing  $0.2^\circ\text{NS}-0.2^\circ\text{EW}$ ). The proposed epicenter is the geometrical mean of all points of the grid for which relations (9) are fulfilled and that solution in this geographical point for which the value of  $q$  has the highest value is taken as the best solution. The adopted magnitude of the ensuing mainshock is the average of the values calculated by relations (3, 4, 5) for the best solution and the corresponding origin time to this solution is considered as a first approximation for the origin time of the ensuing mainshock.

The above described procedure gives satisfactory results for the epicenter and magnitude but only a rough estimation of the origin time. For this reason an alternative technique has been proposed for the determination of the origin time of the mainshock. This technique is based on a precursory seismic excitation, which has been observed to occur in the preshock region at a time that is correlated to the origin time of the oncoming mainshock (Papazachos et al., 2001). This excitation has been recognized by the observation of an abrupt increase (jump) in the relation  $T_i=f(T_c)$  between the calculated identification times,  $T_i$ , and several assumed origin times  $T_c$ , of the oncoming mainshock. This abrupt increase of  $T_i$  occurs when  $T_c$  becomes about equal to the real origin time,  $t_c$ , of the mainshock. The suggestion that this increase of  $T_i$  is due to a seismic excitation in the preshock region, i.e. swarm of preshocks (Evison and Rhoades, 1997) is strongly supported by the observation that it is associated with an increase of the frequency,  $n$ , of preshocks. This increase of  $T_i$  is also associated with a decrease of  $C$  and of  $m$  as well as of the difference,  $t_{13}$ , between the mean of the origin times of the three largest preshocks and the origin time of the mainshock. The decrease of  $C$  and  $m$  is explained by the additional deviation from linearity of  $S(t)$  caused by the seismic excitation while the decrease of  $t_{13}$  is due to the occurrence of at least one of the three largest preshocks during this excitation. Thus, the changes of these five parameters (positive for  $T_i$  and  $n$ , negative for  $C$ ,  $m$ ,  $t_{13}$ ) can be used as measures of the seismic excitation.

Papazachos and his colleagues (2001) considered the relative rate for each parameter (e.g. the ratio of its rate to the maximum absolute value of the rate observed during the whole examined period) and calculated a measure of the seismic excitation, expressed in terms of these five ratios ( $r_i$ ,  $r_n$ ,  $r_c$ ,  $r_m$ ,  $r_t$ ), for each time interval in which the examined period is separated. They considered the average of these five relative values (with change of sign for  $r_c$ ,  $r_m$ ,  $r_t$ ) as such a measure and called it Preshock Excitation Indicator (PEI). Its values vary between 0 and 1 for relative increase of the seismicity (seismic excitation), in respect to the activity predicted by relation (2), and between  $-1$  and 0 for relative decrease of seismicity (seismic quiescence). Thus, by plotting PEI versus  $T_c$  one can determine a time  $T_c=T_{pr}$  for which PEI takes its maximum value. Papazachos and his colleagues (2001) examined thirty-two cases of strong ( $M>6.0$ ) shallow earthquakes in the Aegean area and observed such seismic excitation in thirty of them with an average PEI equal to 0.63 and a standard deviation of 0.19. They also observed that at  $T_c=T_{pr}$ , it is  $T_i\sim t_i$  and  $T_{pr}\sim t_c$ . It means that seismic excitation occurs at about the identification time and that  $T_{pr}$  shows the approximate origin time of the mainshock. The mean difference between the observed origin times,  $t_c$ , of these thirty events and the corresponding  $T_{pr}$  times is almost zero with a standard deviation of 0.9yrs, quite smaller than the equivalent standard deviation for random (uniform) distribution corresponding to the 5-year examined period. In the case when no preshock seismic excitation occurs,  $T_i$  is almost constant and equal

to  $t_i$  and can be used in relations (10, 11) for an estimation of the origin time,  $t_c$ , of the mainshock.

**Table 1.** Information on the eighteen preshock – mainshock sequences studied in this paper.  $t_c$ ,  $\varphi$ ,  $\lambda$ ,  $M$  are the observed origin time, epicenter coordinates and magnitude of the mainshock and  $t_c^*$ ,  $\varphi^*$ ,  $\lambda^*$ ,  $M^*$  are the retrospectively predicted parameters.  $a$  (in km),  $e$ ,  $z$  are the parameters of the elliptical preshock (critical) region,  $M_{min}$  is the minimum preshock magnitude,  $n$  is the number of observations (number of preshocks plus the mainshock) and  $t_s$  is the start year of the preshock sequence ( $=t_c-t_p$ ).

No	$t_c$	$\varphi$ , $\lambda$	$M$	$t_c^*$	$\varphi^*$ , $\lambda^*$	$M^*$	$a$	$e$	$z$	$M_{min}$	$n$	$t_s$
1	1952:12:17	34.4, 24.5	7.0	1952.2	34.9, 24.4	6.9	274	0.90	30	5.2	23	1922
2	1953:03:18	40.0, 27.5	7.4	1953.0	39.4, 27.3	7.6	469	0.95	0	5.6	29	1920
3	1953:08:12	38.1, 20.6	7.2	1952.9	37.9, 20.6	7.3	385	0.95	90	5.3	31	1930
4	1954:04:30	39.1, 22.3	7.0	1954.6	39.1, 22.3	7.3	313	0.95	90	5.3	31	1932
5	1955:07:16	37.6, 27.1	7.0	1954.5	38.0, 26.1	7.0	313	0.95	150	5.2	23	1920
6	1956:07:09	36.6, 26.0	7.5	1955.8	36.4, 25.8	7.6	348	0.70	150	5.6	31	1929
7	1957:04:25	36.5, 28.6	7.2	1957.8	36.1, 28.0	7.4	388	0.95	150	5.4	29	1930
8	1968:02:19	39.5, 25.0	7.1	1968.9	39.6, 25.2	7.0	313	0.95	30	5.3	21	1933
9	1970:03:28	39.2, 29.4	7.0	1970.7	38.8, 29.8	7.2	240	0.80	30	5.3	24	1945
10	1980:07:09	39.3, 22.8	6.5	1979.3	39.3, 22.8	6.1	91	0.70	0	4.5	33	1965
11	1981:02:24	38.2, 22.9	6.7	1982.1	38.0, 23.2	7.0	333	0.95	0	5.2	26	1966
12	1981:12:19	39.0, 25.3	7.2	1981.5	38.8, 25.1	7.3	280	0.80	30	5.3	45	1951
13	1983:01:17	38.1, 20.2	7.0	1983.0	37.2, 20.8	7.2	385	0.95	60	5.3	26	1967
14	1983:07:05	40.3, 27.2	6.4	1982.8	40.0, 27.8	6.3	130	0.90	60	4.6	21	1970
15	1995:05:13	40.2, 21.7	6.6	1996.9	41.0, 21.2	6.7	229	0.95	60	5.0	23	1970
16	1995:06:15	38.4, 22.2	6.4	1995.2	38.6, 22.2	6.7	177	0.80	120	4.9	32	1982
17	1997:10:13	36.5, 22.2	6.4	1998.5	36.5, 22.0	6.6	173	0.90	90	4.8	41	1965
18	1997:11:18	37.6, 20.6	6.6	1997.1	38.2, 20.2	7.0	333	0.95	30	5.3	22	1984

The data used in the present paper concern all shallow mainshocks with  $M \geq 7.0$  which occurred since 1950 and all shallow mainshocks with  $M \geq 6.4$  which occurred since 1980 in the Aegean area, that is, a total of 18 mainshocks. The epicenters of these mainshocks are shown in Fig. (1). Origin times,  $t_c$ , epicenter coordinates  $\varphi^{\circ}_N$ ,  $\lambda^{\circ}_E$  and moment magnitudes for these earthquakes are given in the second, third and fourth columns of table (1). The data used to calculate the Benioff strain have been taken from the complete set (1911-1949  $M \geq 5.2$ , 1950-1964  $M \geq 5.0$ , 1965-2000  $M = 4.5$ ) of the catalog published by Papazachos and his colleagues (2000). The epicenter error is of the order of 15km for earthquakes that occurred after 1965 (when the first network of seismic stations was established in this area) and up to 25-30km for older earthquakes. All magnitudes are equivalent moment magnitudes with typical error of the order of 0.3 and were used to calculate the energy  $E$  (in Joules) that is subsequently used to determine the cumulative Benioff strain according to the equation (Papazachos and Papazachos 2000):

$$\log E = 1.5 M + 4.7 \quad (12)$$

Eighteen areas corresponding to the mainshocks listed in table (1) were considered. Each one of these areas, which includes the epicenter of the corresponding mainshock, is selected to have dimensions of 1.5 degrees in the north-south direction and 1.8 degrees in the east-west direction (~150km). The algorithm described above was applied for each point of a grid (with cells  $0.2^{\circ}NS - 0.2^{\circ}EW$ ), which covers the previously mentioned area, and the best solution is determined. As an example, figure (2) shows the time variation of the cumulative Benioff strain for the best solution of the April 1954 earthquake (number 4 in table 1).

## RESULTS

Figures (3a, b, c) show the eighteen elliptical regions corresponding to the best solutions determined by the procedure described above. The star in each case shows the center of the

ellipse, which is the geographical point for which the best solution (highest  $q$  value) holds and which is considered as the predicted epicenter of the earthquake. The large black circle shows the observed epicenter of the mainshock and the small circles denote the epicenter of the preshocks, as these epicenters are listed in the catalogues used in this study. The geographical coordinates ( $\varphi^*$ ,  $\lambda^*$ ) of the center of each ellipse (predicted epicenter), the length,  $a$  (in km), of the big axis of the ellipse, its ellipticity,  $e$ , and the azimuth,  $z$ , of its big axis are given on table (1). In the same table the minimum magnitude,  $M_{\min}$ , of the preshocks, the number,  $n$ , of preshocks and the start time,  $t_s$  ( $=t_c-t_p$ ), of each sequence are also given.

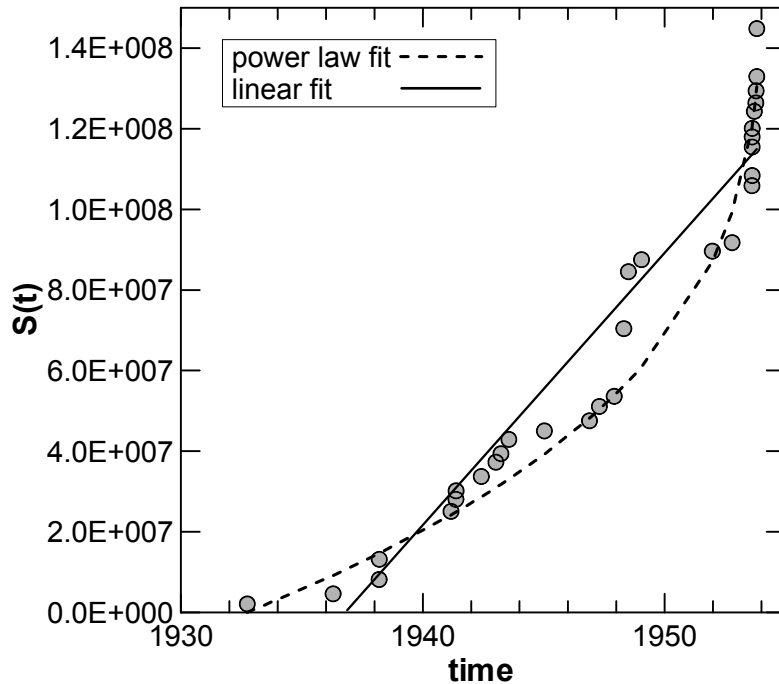
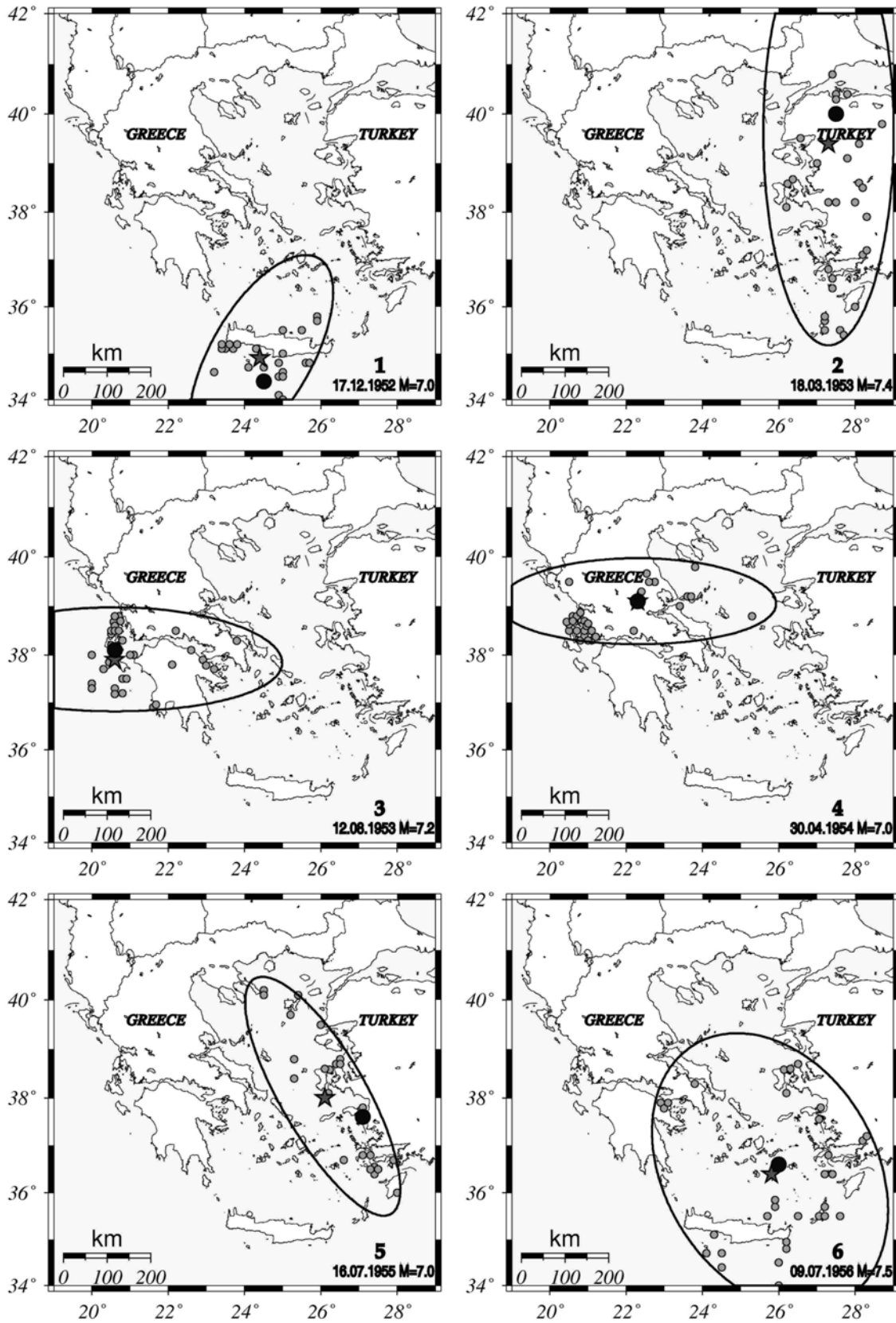


Figure 2. Time variation of the cumulative Benioff strain,  $S(t)$ , for the best solution of April 1954 ( $M=7.0$ ) earthquake (number 4 in table 1).

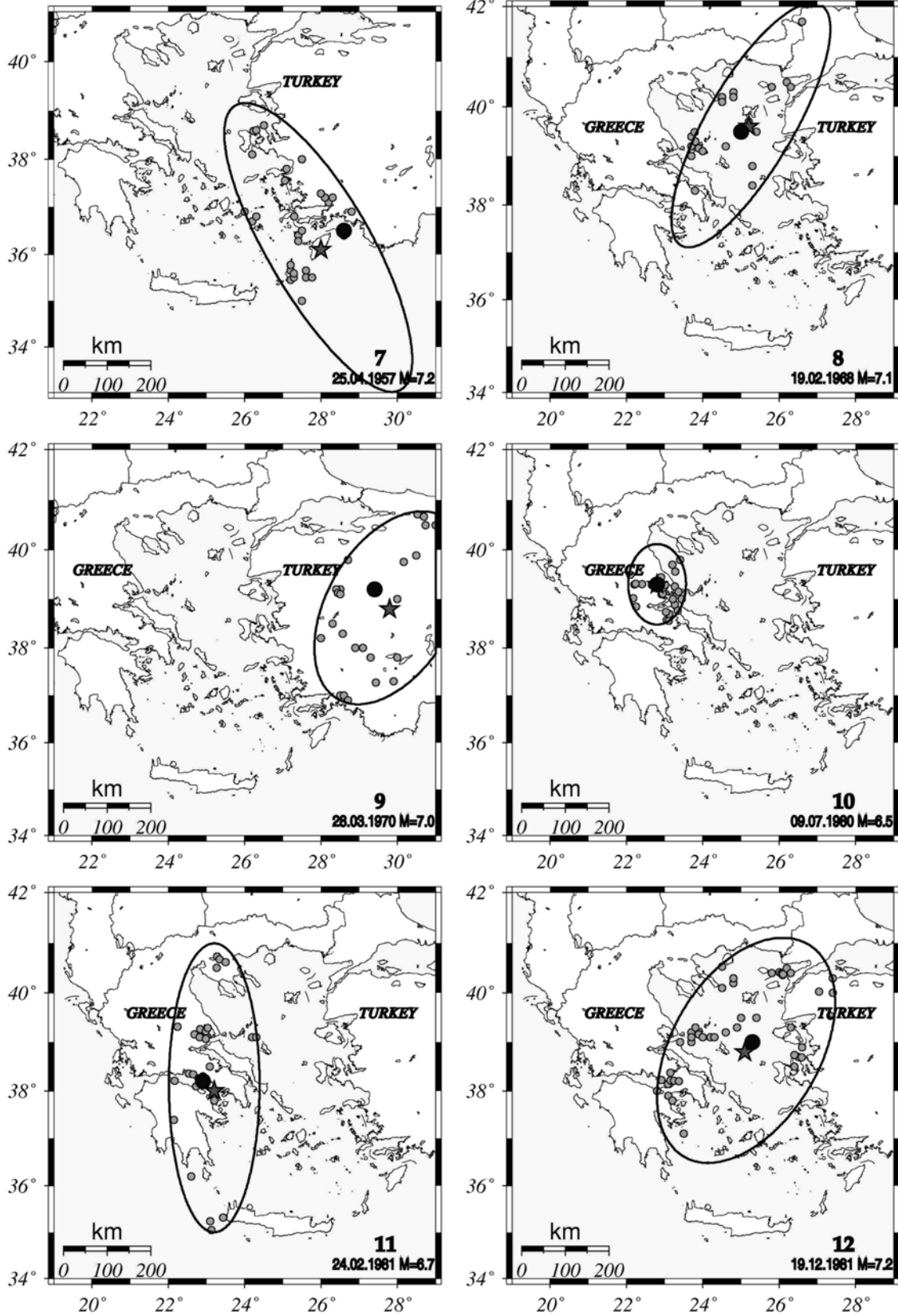
An interesting feature of the preshock distribution in figure (3) is that the epicenter of the mainshock is usually in an area where no cluster of preshock epicenters is observed. This supports the idea that preshocks occur in smaller faults when tectonic stress is at relatively low level and their occurrence contributes to the redistribution of stress in the preshock (critical) region. This physical process leads to an increase of the tectonic stress in the mainshock fault and to the generation of the mainshock.

In table (1) the predicted magnitude,  $M^*$ , is also given. This is the average of the three magnitudes calculated by relations (3, 4, 5) for the best solution of each of the eighteen cases. Thus, having the predicted epicenter coordinates ( $\varphi^*$ ,  $\lambda^*$ ) and the predicted magnitude,  $M^*$ , for the mainshock of each sequence, the Preshock Excitation Indicator (PEI) can be determined as a function of assumed values,  $T_c$ , of the origin time of the mainshock. Calculations of PEI have been made in steps of 3 months and for an interval of four years or larger for  $T_c$ . Figures (4a, b, c) show the variation of the calculated PEI values as a function of  $T_i$  for each of the eighteen sequences. Axis  $T_i$  starts at the average value of PEI for each sequence. The standard deviation,  $\sigma$ , from the mean has been calculated and the interval  $\pm 2\sigma$  is shown by the two dashed lines for each plot in figures (4a, b, c). It is clear that in all eighteen cases a pronounced positive value of PEI is observed, which is well above the two standard deviations value. The value of  $T_c$  corresponding to the maximum value of PEI is considered as the predicted origin

(a)



(b)





(c)

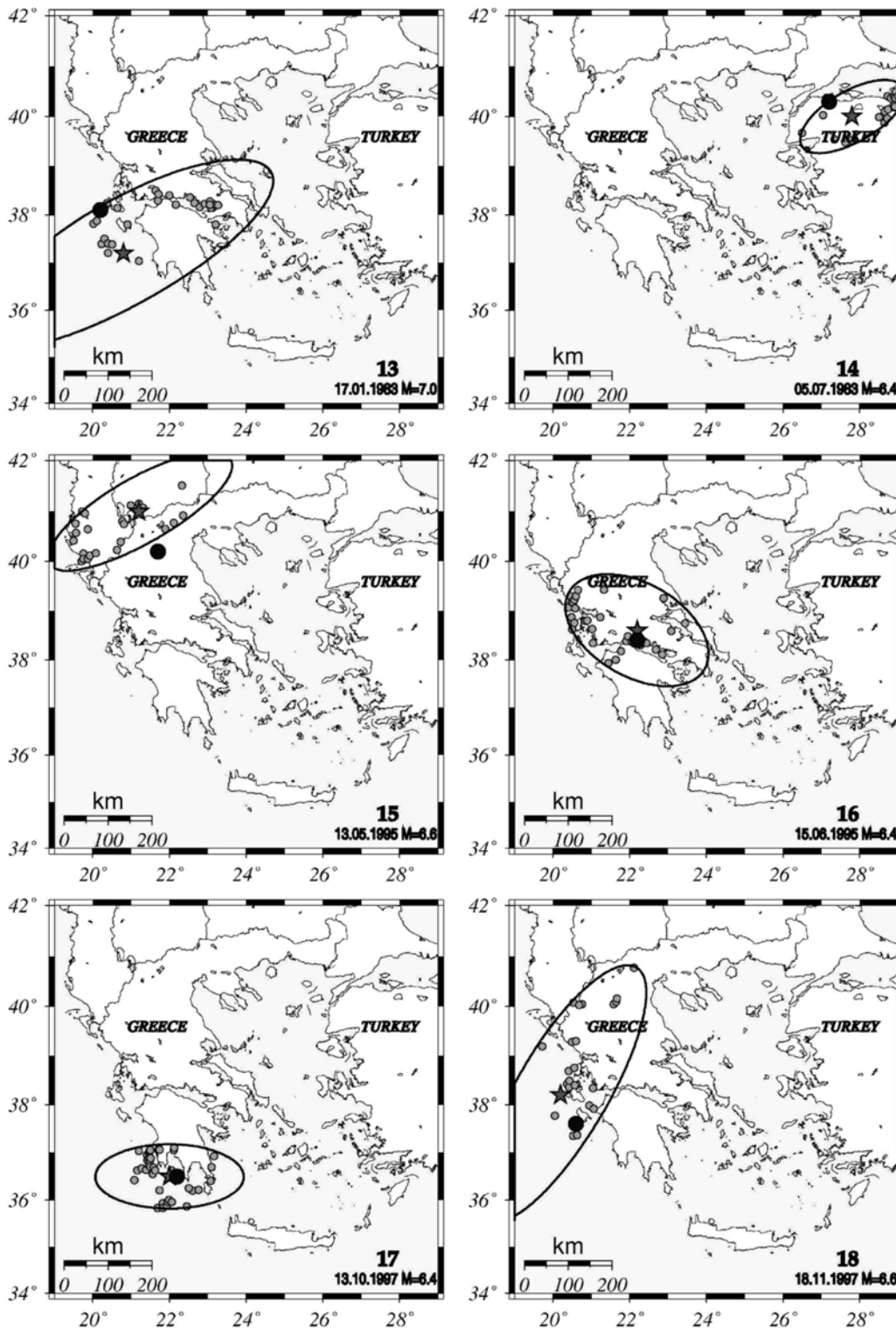


Figure 3 (a), (b), (c). The elliptical critical regions of the eighteen mainshocks along with the epicenters of their respective preshocks. Stars denote the centers of the ellipses, which correspond to the grid points with the best solutions and hence implying the epicenters of the expected earthquakes, whereas the solid circles denote the observed mainshock epicenters.

time,  $t_c^*$ , which is also given on table (1). The arrows in figures (4a, b, c) show the value of observed origin time,  $t_c$ , of the mainshock.

From table (1) it comes out that the distance between the observed epicenter ( $\varphi, \lambda$ ) and the predicted epicenter ( $\varphi^*, \lambda^*$ ) varies between 14km and 100km with an average equal to 48km and a standard deviation equal to 33km. This result suggests that there is a high probability (>90% confidence) for the epicenter of an ensuing mainshock to be within a distance of about 110km from the predicted one.

The difference between the observed mainshock magnitude,  $M$ , and the retrospectively predicted one,  $M^*$ , varies between  $-0.4$  and  $0.4$  with an average equal to  $-0.11$  and a standard deviation equal to  $0.19$ . It means that the uncertainty in calculating the magnitude of an ensuing mainshock can be less than  $0.4$  with high probability (>90% confidence).

Table (1) also shows that the difference between the observed,  $t_c^*$ , and estimated origin time varies between  $-1.50$  and  $1.26$  with a mean equal to  $0.10$  and a standard deviation equal to  $0.77$  years. Hence, there is a high probability that the origin time of an ensuing mainshock to be predicted with an error  $\pm 1.5$  years (>90% confidence).

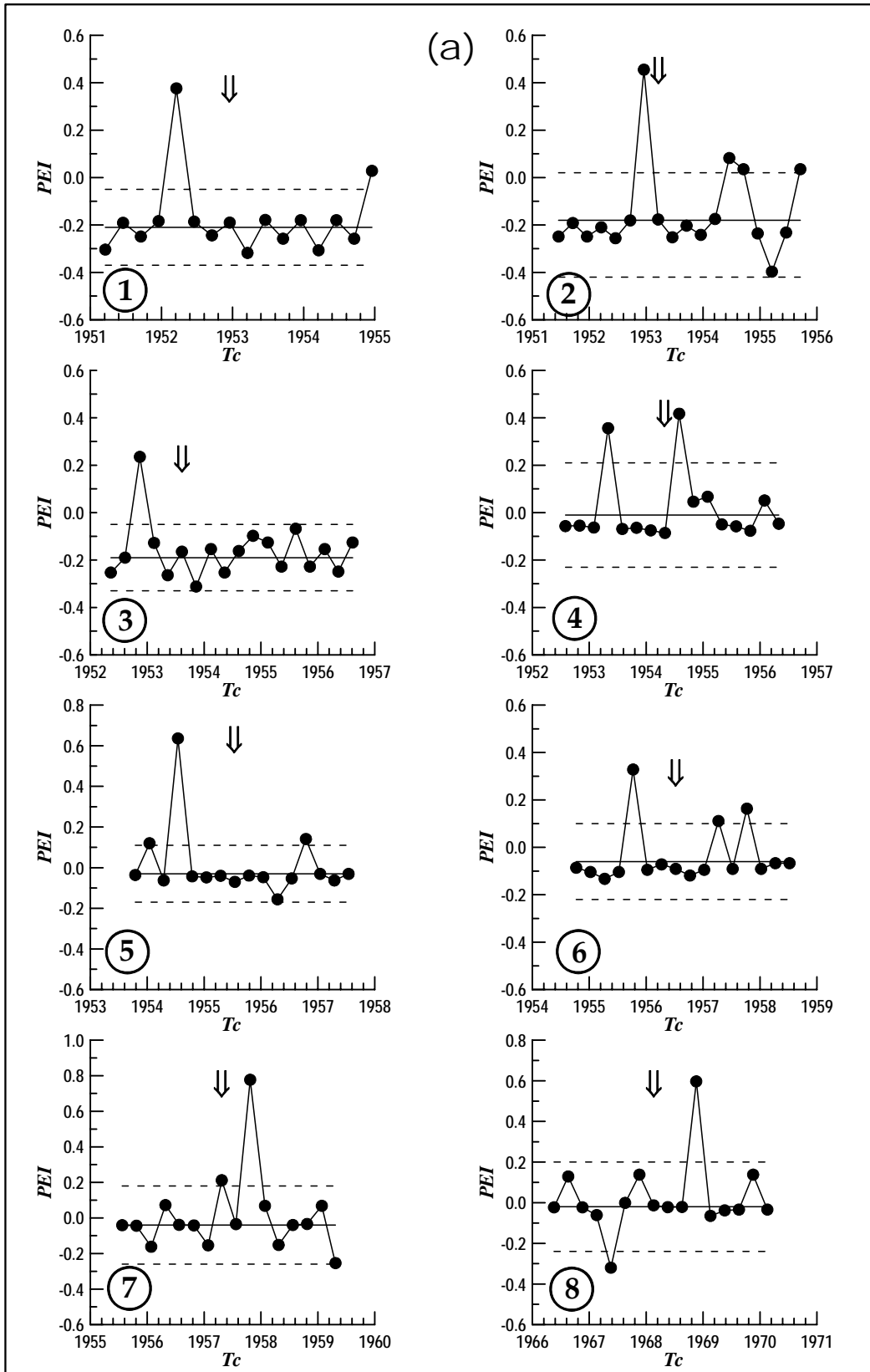
## DISCUSSION

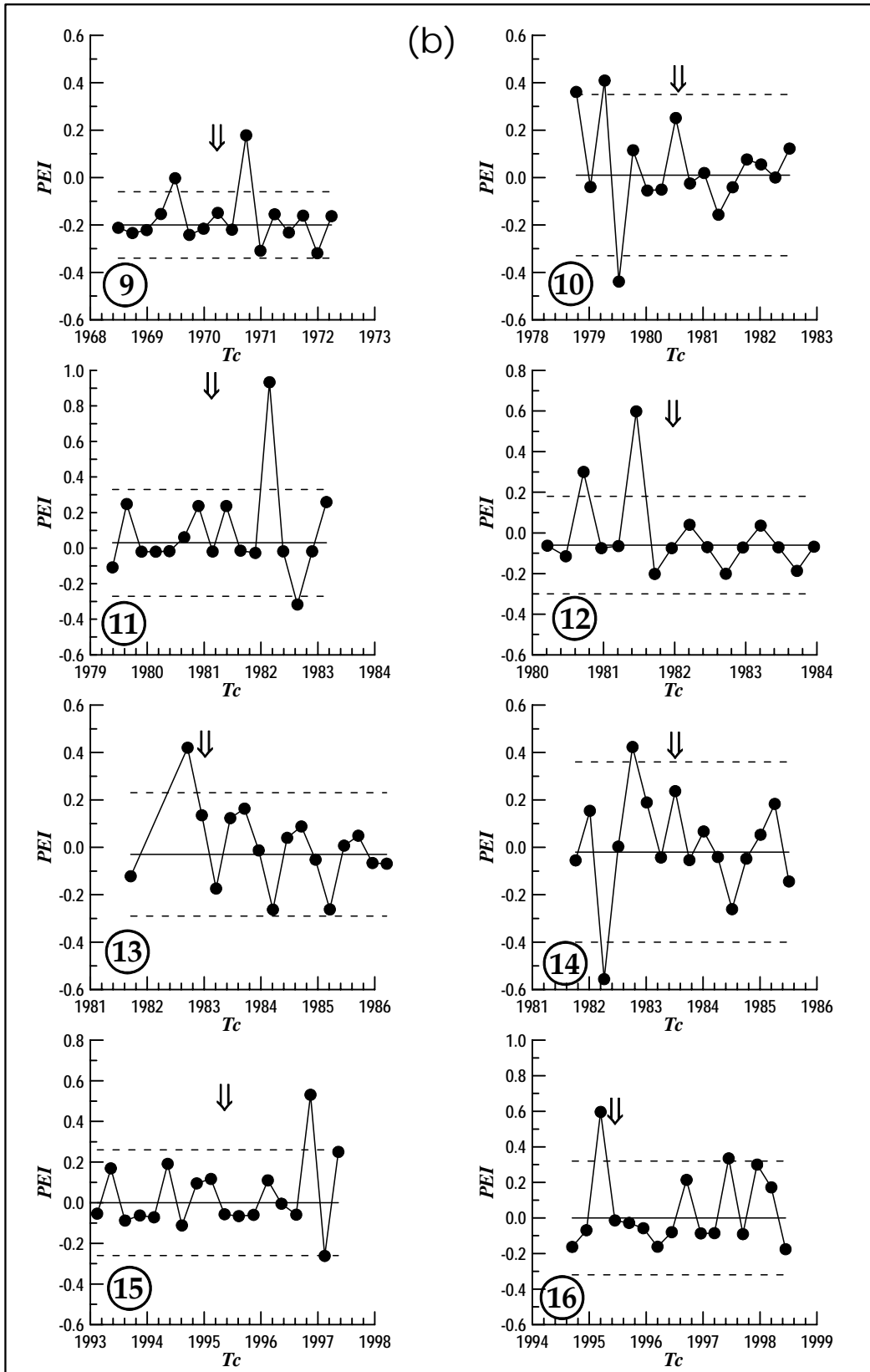
The procedure described above can be probably applied to predict future strong mainshocks. There are, however, still some problems, which limit its application. Specifically, this procedure cannot be easily applied to predict strong preshocks or strong postshocks, that is, earthquakes that occurred up to some years before or after a mainshock and in a small distance from its epicenter. This is due to the fact that their critical (preshock) regions are parts of the critical region of the mainshock and that part of their preshock time coincides with a part of the preshock time of the mainshock. Thus, their preshock region and time are not easily distinguishable and for this reason cannot be easily defined. Moreover, regarding the preshock time, the problem is more difficult in areas of low seismicity where preshock times are quite large.

In some cases it is difficult to uniquely define one point of an investigated area, which corresponds to a minimum value of  $C$ , because in a neighboring area another earthquake is also under "preparation", hence there is an interference of the two preshock processes. A correct interpretation of such kind of data is possible but the uncertainties in the predicting parameters are high in such cases.

We have found no cases of strong mainshocks ( $M > 6.0$ ) that occurred in this area during the last two decades, when the most reliable data are available, which have not been preceded by accelerated seismicity. There are, however, examples of strong earthquakes in other areas, which have not been preceded by such seismicity (Jaume and Sykes, 1999). For this reason such cases cannot be excluded for the region examined in the present work. It must be noted that the cases of earthquakes without preshock accelerating seismic deformation must be rare, if any, in this region. Moreover, we have not observed any case of accelerating seismicity in this region, which has not been followed by a strong mainshock. Therefore, we cannot exclude such cases, which can lead to false alarms. The present method, however, puts several constraints to the final solution and for this reason false alarms, if any, must be rare.

Although there are still several problems related to the possibility for real predictions of future mainshocks by the method described above, it has the advantage that, in addition to the use of the relation (2) which has also been used for this purpose by previous investigators, it makes use of several other properties of the critical earthquake model (e.g. relations 3, 4, 5, 6, 7, 8, 9, 10, 11). Furthermore, this method allows the possibility for a continuous monitoring of the identified critical region during the few years period between the identification time,  $t_i$ , and the origin time,  $t_c$ , of the mainshock (monitoring for other seismic, geophysical and geodetic precursors) and for taking preparedness measures to reduce the social effects of ensuing mainshocks. It is worth mentioning that the application of the method described in this paper has already resulted in the identification of an elliptical critical region in the North Aegean where nine months later a strong earthquake (26.7.2001,  $M=6.4$ ) occurred with its basic focal parameters to be well within the space-time-magnitude window specified (Karakaisis et al. 2001).





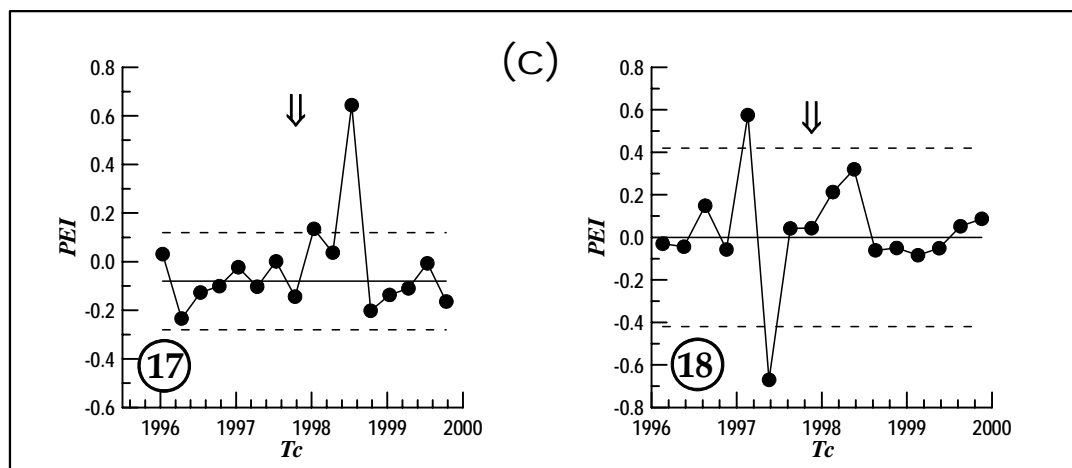


Figure 4 (a), (b), (c). The Preshock Excitation Indicator (PEI) as a function of several assumed origin times,  $T_c$ , of the mainshocks for each case. The arrows indicate the observed origin times of these mainshocks. Dashed lines correspond to  $\pm 2\sigma$  values of PEI for each case.

#### ACKNOWLEDGMENTS

This study would not have been possible without the continuous stimulation of the Professor Emeritus Basil Papazachos to whom we express our many thanks. The GMT software (Wessell and Smith, 1995) was used to generate some of the maps of this study. This work has been partially supported by the Greek Planning and Protection Organization (OASP), (Res. Comm. AUTH project 20242) and is a Geophysical Laboratory contribution number #0601/2002.

#### REFERENCES

- Bowman, D.D., Quillon, G., Sammis, C.G., Sornette, D. and Sornette, A., 1998. An observational test of the critical earthquake concept, *J. Geophys. Res.*, 103, 24359-24372..
- Bufe, C.G. and Varnes, D.J., 1993. Predictive modeling of the seismic cycle of the great San Francisco Bay region, *J. Geophys. Res.*, 98, 9871-9883.
- Bufe, C.G., Nishenko, S.P. and Varnes, D.J., 1994. Seismicity trends and potential for large earthquake in the Alaska – Aleutian region, *Pure Appl. Geophys.*, 142, 83-99.
- Ellsworth, W.L., Lind, A.G., Prescott, W.H. and Herd, D.G., 1981. The 1906 San Francisco earthquake and the seismic cycle. In *Earthquake Prediction: An International Review* (eds. Simpson, D.W. and Richards, P.G.), AGU, Washington, D.C. 1981, pp. 126-140.
- Evison, F.F. and Rhoades, D.A., 1997. The precursory earthquake swarm in New Zealand, *N. Z. Journal of Geology and Geophysics*, 40, 537-547.
- Gutenberg, B., and Richter, C.F., 1954. *Seismicity of the Earth and Associated Phenomena* (Hafner, New York 1954).
- Huang, Y., Saleur, H., Sammis, C. and Sornette, D., 1998. Precursors, aftershocks, criticality and self organized criticality, *Europhys. Lett.*, 41, 43-48.
- Jaume, S.C. and Sykes, L.R., 1999. Evolving toward a critical point: A review of accelerating seismic moment/energy release prior to large and great earthquakes, *Pure Appl. Geophys.*, 155, 279-306.
- Jaume, S. C., Weatherley, D. and Mora, P., 2000. Accelerating seismic energy release and evolution of event time and size statistics: results from two heterogeneous cellular automaton models, *Pure appl. geophys.*, 157, 2209-2226.
- Karakaisis, G.F., Kourouzidis, M.C. and Papazachos, B.C., 1991. Behavior of seismic activity during a single seismic cycle. In *Earthquake prediction: state of the art, Strasbourg, France, 15-18 October 1991*, 47-54.
- Karakaisis, G. F., Papazachos, C. B., Savvaidis, A. S. and Papazachos, B. C., 2001. Accelerating seismic crustal deformation in the North Aegean Trough, Greece, *Geophys. J. Int.* (in press).

- Knopoff, L., Levshina, T., Keilis-Borok, V.J. and Mattoni, C., 1996. Increased long range intermediate magnitude activity prior to strong earthquakes in California, *J. Geophys. Res.*, 101, 5779-5796.
- Mogi, K., 1969. Some features of recent seismic activity in and near Japan (2). Activity before and after great earthquakes, *Bull. Earthquake Res. Inst. Univ. Tokyo*, 47, 395-417.
- Papadopoulos, G.A., 1986. Long - term earthquake prediction in western Hellenic arc, *Earthquake Pred. Res.*, 4, 131-137.
- Papazachos, C.B., 2001. An algorithm for intermediate term earthquake prediction by the accelerated seismic deformation method. *2<sup>nd</sup> Hellenic Conference on Earthquake Engineering and Engineering Seismology, 28-30 November 2001*, 1-10.
- Papazachos, B. and Papazachos, C., 2000. Accelerated preshock deformation of broad regions in the Aegean area, *Pure Appl. Geophys.*, 157, 1663-1681.
- Papazachos, C. and Papazachos, B., 2001. Precursory accelerated Benioff strain in the Aegean region, *Annali di Geofisica*, 44, 461-474, 2001.
- Papazachos, B.C., Comninakis, P.E., Karakaisis, G.F., Karacostas, B.G., Papaioannou, Ch.A., Papazachos, C.B. and Scordilis, E.M., 2000. A catalogue of earthquakes in Greece and surrounding area for the period 550BC-1999, *Publ. Geoph. Lab. Univ. of Thessaloniki*, 1, 333pp. (also at <http://geohazards.cr.usgs.gov/iaspei/europe/greece/the/catalog.txt>).
- Papazachos, B.C., Karakaisis, G.F., Papazachos, C.B., Scordilis, G.F. and Savvaidis, A.S., 2001. A method for estimating the origin time of an ensuing mainshock by observations of preshock crustal seismic deformation, *Bull. Geol. Soc. Greece*, 34, 1573-1579.
- Papazachos, C.B., Karakaisis, G.F., Savvaidis, A.S. and Papazachos, B.C., 2002. Accelerating seismic crustal deformation in southern Aegean area, *Bull. Seism. Soc. Am.*, (in press).
- Raleigh, C.B., Sieh, K., Sykes, L.R., and Anderson, D.L., 1982. Forecasting Southern California earthquakes, *Science*, 217, 1097-1104.
- Saleur, H., Sammis, C.G., and Sornette, D., 1996. Discrete invariance, complex fractal dimensions, and long periodic fluctuations in seismicity, *J. Geophys. Res.*, 101, 17661-17677.
- Sornette, A., and Sornette, D., 1990. Earthquake rupture as a critical point. Consequences for telluric precursor, *Tectonophysics*, 179, 327-334.
- Sornette, D. and Sammis, C.G., 1995. Complex critical exponents from renormalization group theory of earthquakes: Implications for earthquake prediction, *J. Phys. I.*, 5, 607-619.
- Sykes, L.R. and Jaume, S., 1990. Seismic activity on neighboring faults as long term precursors to large earthquakes in the San Francisco Bay Area, *Nature*, 348, 595-599.
- Tocher, D., 1959. Seismic history of the San Francisco bay region, *Calif. Div. Mines Spec. Rep.*, 57, 39-48.
- Turcotte, D.L., 1999. Seismicity and self-organized criticality, *Phys. Earth. Planet. Interiors*, 111, 275-293.
- Tzanis, A., Vallianatos, F. and Makropoulos, K., 2000. Seismic and electric precursors to the 17.1.1983, M7 Kefallinia Earthquake, Greece: Signatures of a SOS System, *Phys. Chem. Earth*, 25, 281-287.
- Varnes, D.J., 1989. Predicting earthquakes by analyzing accelerating precursory seismic activity, *Pure Appl. Geophys.*, 130, 601-686.
- Wessel, P., and Smith, W., 1995. New version of the Generic Mapping Tools, *EOS Trans. Amer. Geophys. U.*, 76, 329.
- Yang, W., Vere-Jones, D. and Li, M., 2001. A proposed method for locating the critical region of a future earthquake using the critical earthquake concept, *J. Geophys. Res.*, 106, 4121-4128.